Exploring 1,2-Hydrogen Shift in Silicon Nanoparticles: Reaction Kinetics from Quantum Chemical Calculations and Derivation of Transition State Group Additivity Database

ARTICLE *in* THE JOURNAL OF PHYSICAL CHEMISTRY A · SEPTEMBER 2009

Impact Factor: 2.69 · DOI: 10.1021/jp9062516 · Source: PubMed

4 AUTHORS, INCLUDING:

Andrew Adamczyk
Independent Researcher
14 PUBLICATIONS **163** CITATIONS
SEE PROFILE

Bryan Marin
Ghent University
401 PUBLICATIONS **4,825** CITATIONS
SEE PROFILE

Exploring 1,2-Hydrogen Shift in Silicon Nanoparticles: Reaction Kinetics from Quantum Chemical Calculations and Derivation of Transition State Group Additivity Database

Andrew J. Adamczyk,[†] Marie-Francoise Reyniers,[‡] Guy B. Marin,[‡,§] and Linda J. Broadbelt*,[†]

Department of Chemical and Biological Engineering, Northwestern University, Evanston, Illinois 60208, Laboratory for Chemical Technology, Ghent University, Ghent, B-9000, Belgium

Received: July 2, 2009; Revised Manuscript Received: August 20, 2009

Accurate rate coefficients for 35 1,2-hydrogen shift reactions for hydrides containing up to 10 silicon atoms have been calculated using G3//B3LYP. The overall reactions exhibit two distinct barriers. Overcoming the first barrier results in the formation of a hydrogen-bridged intermediate species from a substituted silylene and is characterized by a low activation energy. Passing over the second barrier converts this stable intermediate into the double-bonded silene. Values for the single event Arrhenius pre-exponential factor, $\tilde{A}$, and the activation energy, E_a, were calculated from the G3//B3LYP rate coefficients, and a group additivity scheme was developed to predict $\tilde{A}$ and E_a. The values predicted by group additivity are more accurate than structure/reactivity relationships currently used in the literature, which rely on a representative $\tilde{A}$ value and the Evans−Polanyi correlation to predict E_a. The structural factors that have the most pronounced effect on $\tilde{A}$ and E_a were considered, and the presence of rings was shown to influence these values strongly.

Introduction

Chemical vapor deposition (CVD) is an important method by which semiconductors are fabricated industrially. Pyrolysis of the feed gas, typically SiH_4 or Si_2H_6, is the standard protocol to create polycrystalline silicon, but the performance of microelectronics created via this process can be compromised by polymerization of silicon hydrides in the gas phase.[1] Nanoparticles that are formed deposit on the growing semiconductor surface, leading to point defects. Optimizing reactor design and process conditions plays a key role in the control of nanoparticle formation. For instance, the kinetics of 1,2-hydrogen shift (Figure 1), which is a key reaction class in silane pyrolysis, has been shown to be highly sensitive to variations in temperature, pressure, and bath gas.[2,3] A clear understanding of the routes to nanoparticle formation will also allow for the control of technologies where nanoparticles are intentionally formed.[4,5] These technologies create tailored nanoparticles for optoelectronic and biophotonic applications[6] in which the size and crystallinity of the particles play an integral role.

The 1,2-hydrogen shift reaction for silicon hydrides is a route by which unstable substituted silylenes with a divalent center can be stabilized by the formation of a silene with a π bond.[7] Stabilization of a divalent silicon center was first experimentally validated by the synthesis of a Si═Si bond by West and Fink[8] in 1981. Others have since studied and confirmed the importance of this reaction pathway theoretically[2,7,9−16] and experimentally[17−22] for the isomerization of silylsilylene to disilene. Interest in π-bonded silicon atoms extends beyond Si−H systems to chlorosilicon hydrides,[15] organosilicon species,[23] and even interstellar systems.[24] Nonetheless, detailed exploration of the 1,2-hydrogen shift reaction of substituted silylenes has not been extended beyond species with two silicon atoms, and it is precisely this information that is necessary to describe nanoparticle growth kinetics.

Recently, automated network generation techniques[25−31] have emerged that allow the kinetics of silicon nanoparticle formation to be described at the mechanistic level.[3] Rate coefficients must be estimated for every elementary step comprising the mechanistic model, and kinetic correlations are used to make this tractable. One common method for predicting E_a is the Evans−Polanyi correlation[32] depicted in eq 1, where E_0 and γ are parameters that are determined from linear regression against experimental or theoretical values and are constant for a given reaction class. For the 1,2-hydrogen shift reaction, Evans−Polanyi parameters of $E_o = 7.5$ kcal mol^{-1}, $\gamma = 0$ (substituted silylene to silene), $\gamma = 1$ (silene to substituted silylene),[3,15] and a single event value of $\tilde{A} = 1 \times 10^{13}$ s^{-1} have been used.[1] However, it has not been demonstrated that these literature values are accurate for an isomerization reaction involving a larger number of silicon atoms and a variety of substituents near the reactive center.

$$E_a = E_0 + \gamma \Delta H_{Rxn} \tag{1}$$

An alternative approach for estimating kinetic parameters is transition state group additivity (TSGA). Inspired by the pioneering group additivity methods developed by Benson for thermochemical property estimation,[33] which have been successfully applied over a wide range of temperatures to silicon hydrides for S, C_p, and ΔH_f by Wong et al.,[34] Sumathi et al.[35−37] first applied group additivity to the thermodynamic properties of the transition state for rate coefficient prediction of hydrogen abstraction reactions. Saeys et al.[38,39] and Sabbe et al.[40] then improved the method for reaction classes governing hydrocarbon chemistry by allowing group additivity to calculate the *differences* in properties between the transition state and the reactant. The basic method treats reactions for which predictions of kinetic parameters are desired as perturbations to a reference reaction. This approach builds on the work by Willems and

* Corresponding author. E-mail: broadbelt@northwestern.edu.
[†] Northwestern University.
[‡] Ghent University.
[§] E-mail: guy.marin@ugent.be.

10.1021/jp9062516 CCC: $40.75
Published on Web 09/21/2009

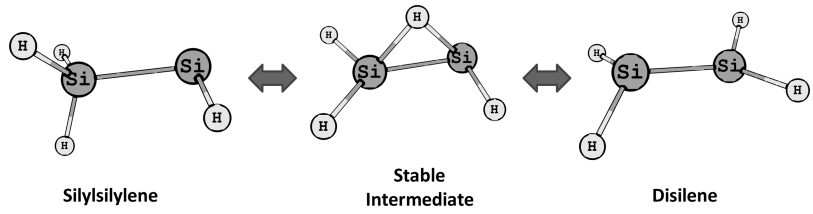

Figure 1. Reference reaction for the 1,2-hydrogen shift.

TABLE 1: Training Set Reactions

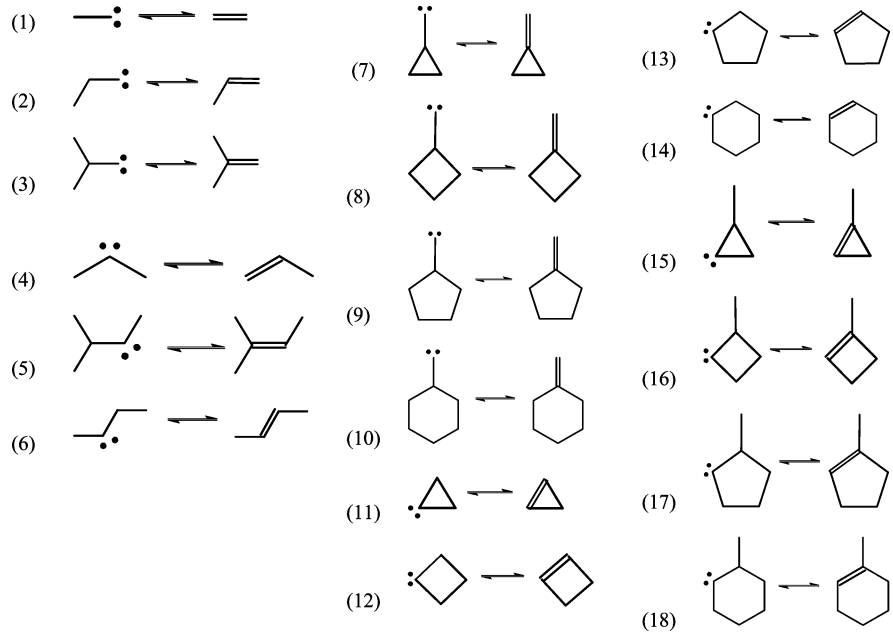

Froment,[41,42] who predicted pre-exponential factors and activation energies on the basis of structural deviations of the reactants from a reference reaction using a combination of transition state theory, statistical thermodynamics, and group additivity for thermodynamic properties to describe the steam cracking of hydrocarbons. However, no quantum chemical calculations were used to explicitly calculate $\tilde{A}$ and E_a for each single event. Saeys et al.[38,39] extended their approach to the prediction of activation energies for hydrogen abstraction and radical addition/β-scission reactions based on explicit transition state geometries calculated using quantum chemistry (CBS-QB3). Sabbe and co-workers[40] then extended the transition state group additivity method to the prediction of pre-exponential factors for radical addition/β-scission reactions using CBS-QB3, as well. Truong and co-workers[43,44] adopted a similar approach for predicting rate coefficients of hydrogen abstraction reactions that they termed reaction class transition state theory, which relies on a reference reaction, the reaction energy, and the differential barrier height.

The TSGA method possesses several advantages that should interest kineticists seeking parameters for the 1,2-hydrogen shift reaction in silicon hydrides. This method requires a number of parameters similar to that of the Evans−Polanyi correlation, but (1) allows one to gain insight into the changes in the reactive center during reaction, (2) implements multiple values of $\tilde{A}$ for each reaction class, and (3) circumvents the need to calculate accurate standard enthalpies and Gibbs free energies of reaction as required for the Evans−Polanyi correlation and reverse rate coefficient, respectively. The structure of the reactant(s) and product(s) for a given reaction class is sufficient to allow accurate kinetic parameter estimation.

This paper presents the first extension of the TSGA approach to silicon hydride chemistry and specifically examines the 1,2-hydrogen shift reaction for molecules containing up to 10 silicon atoms. All elementary steps studied involved monofunctional compounds; that is, molecules containing either a π bond or divalent center, but not both. Species containing rings with up to 6 silicon atoms were considered. The composite method of G3//B3LYP[45] was used to calculate the electronic energy, and then statistical thermodynamics was applied to all reactants and transition states to incorporate temperature effects. Single event rate coefficients at 1 atm and 298−1500 K were calculated using transition state theory (TST), and then activation energies, E_a, and single event pre-exponential factors, $\tilde{A}$, were regressed. A training set of E_a and $\tilde{A}$ values was used to regress transition state group additivity (TSGA) values. These group additivity parameters were then validated against reactions not used in the training set. Last, a comparison of the rate coefficients predicted by the Evans−Polanyi correlation and those calculated using G3//B3LYP and TSGA was performed.

Computational Methodology

Quantum Chemical Calculations, Transition State Theory, and Statistical Thermodynamics. Quantum chemical calculations were performed with Gaussian 03[46] for all the reactions summarized in Tables 1 (training set) and 2 (validation set). All electronic energies for substituted silylenes, silenes, transition states, and intermediates were calculated using the G3//B3LYP method,[45] which uses B3LYP geometries and higher-level corrections based on single point energies. Geometries and harmonic frequencies of the lowest energy conformers were

TABLE 2: Validation Set Reactions

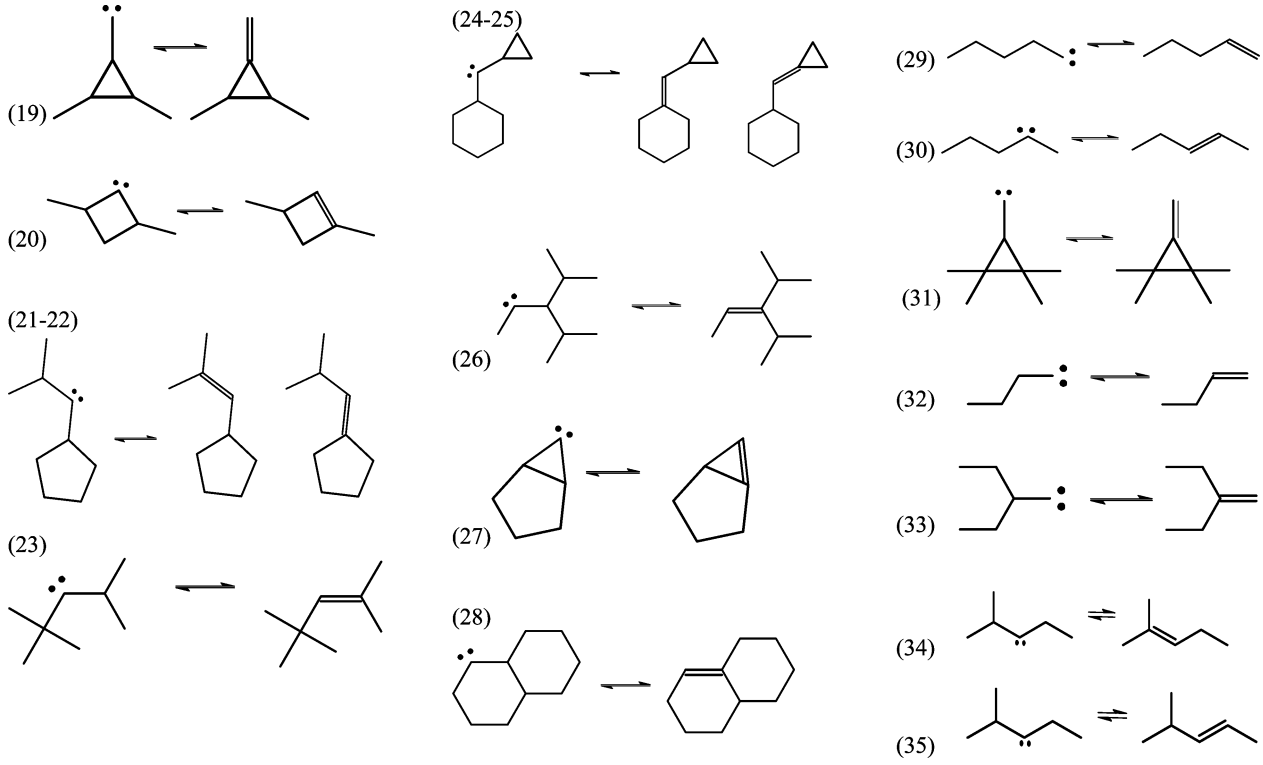

determined at the B3LYP/6-31G(d) level. The harmonic frequencies and zero point energy were scaled by factors of 0.96 and 0.98, respectively, to account for anharmonicity in the normal vibrational modes as suggested by Scott and Radom.[47] The Cartesian coordinates and frequencies for all species can be found in the Supporting Information.

Using conventional statistical thermodynamics, partition functions based on the harmonic oscillator and rigid rotor approximations were used to calculate thermodynamic and kinetic properties as a function of temperature. Attempts were made to quantify anharmonic effects using the one-dimensional hindered rotor approximation. However, one-dimensional scans about the transitional bond (Figure 1) present in substituted silylenes resulted in the formation of stable species that were actually distinct isomers. For example, rotation about the reactive center for $H_3SiH_2SiH_2SiSi{:}SiH_3 \leftrightarrow H_3SiH_2SiHSi{=}SiHSiH_3$ resulted in formation of 1,3- or 1,4-bridged intermediates (Figure 2). Katzer et al.[48] examined anharmonic effects and suggest the formation of a weak dative bond between the divalent silicon atom of a substituted silylene and its neighbor (Figure 3), which raises the barrier of rotation for systems containing rigid bi- and polycyclic character and, thus, decreases contributions of 1-D hindered rotations. However, for situations in which one internal rotation is lost during reaction, such as would take place for 1,2-hydrogen shift, the effect on ΔG_{Rxn} is very small over the temperature range of this study.[49] Thus, no one-dimensional hindered rotation corrections were applied for the 1,2-hydrogen shift reactions in this study.

On the basis of studies of dihydrogen reacting with silicon-derived radicals, Crosby and Kurtz[50] suggest that the MPW1K functional provides superior prediction of kinetics compared to B3LYP. Interestingly, calculations using MPW1K/6-31++G** found transition states for both barriers that lead to a common stable intermediate but only saddle points for silylsilylene and disilene. To benchmark the G3//B3LYP method used in this theoretical study, Weizmann-1 calculations[51] were performed and found to be in excellent agreement with the G3//B3LYP results. For example, values for the rate coefficient for the isomerization of silylsilylene to disilene were within a factor of 1.30 over the 750−1200 K range. In addition, G3//B3LYP was a reasonable choice because the TSGA database is intended to be used in conjunction with an existing G3//B3LYP database developed by our group[34] for the estimation of silicon hydride thermochemical properties.

Transition states were found using the potential energy surface interpolation method QST3. The imaginary frequency of each

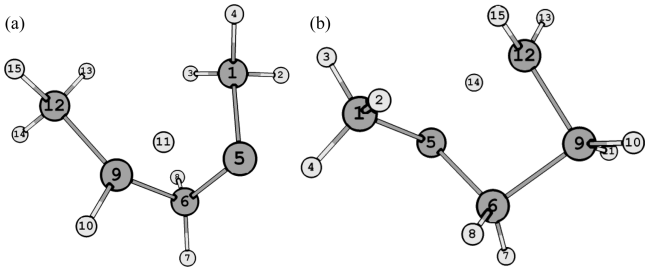

Figure 2. B3LYP/6-31G(d) optimized geometries of intermediate formed from the internal rotation of the reactive center for reaction 30: (a) 1,3-bridged and (b) 1,4-bridged species.

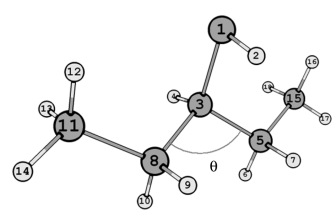

θ (degrees)	Wiberg Bond Index Si_1-Si_3
107	1.00
85	1.01
60	1.11

Figure 3. B3LYP/6-31G(d) bond orders (Si_1-Si_3) for the substituted silylene of reaction 33 as a function of the $Si_5-Si_3-Si_8$ bond angle θ.

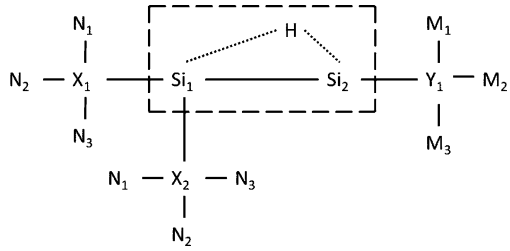

Figure 4. Second transition state of 1,2-hydrogen shift reaction where the dashed box is the reactive center. X and Y are primary contributions. N and M are secondary interactions.

transition state was animated, and intrinsic reaction coordinate following was carried out to confirm that the normal vibrational mode pertained to the reaction coordinate of interest. Conventional TST[52] was then used to calculate rate coefficients according to the macroscopic formulation in eq 2 at 1 atm assuming an ideal gas,

$$k^{\mathrm{TST}}(T) = n_{\mathrm{d}}\tilde{k} = n_{\mathrm{d}}\Lambda \exp\left(\frac{\Delta S^{\neq}}{R}\right)\exp\left(\frac{-\Delta H^{\neq}}{RT}\right) \qquad (2)$$

where Λ, defined in eq 3,

$$\Lambda = \kappa(T)\frac{k_{\mathrm{B}}T(V_{\mathrm{m}}{}^{0})^{-\Delta n}}{h} \qquad (3)$$

is the single event rate coefficient; $\kappa(T)$ is the Wigner tunnelling correction[53] at temperature T; k_{B} is Boltzmann's constant; h is Planck's constant; $V_{\mathrm{m}}{}^{0}$ is the standard molar volume; R is the ideal gas constant; $\Delta S^{\neq}$ is the entropy of activation; $\Delta H^{\neq}$ is the enthalpy of activation; Δn is the change in the number of moles going from the reactant to the transition state (i.e., zero in both directions for isomerization); and n_{d} is the reaction path degeneracy, or number of single events. $\Delta H^{\neq}$ and $\Delta S^{\neq}$ are calculated using standard formulae.[52]

The single event parameters of the Arrhenius relationship, $\tilde{A}$ and E_{a}, were obtained by fitting ln k versus T^{-1} over the temperature range 298−1500 K. This procedure was performed automatically using the CalcK script developed by our group.[54] Arrhenius behavior was obeyed well; for example, reaction 1 had a linear regression coefficient equal to 1.

TSGA Model and Application to 1,2-Hydrogen Shift Reactions. Transition state group additivity was adapted to describe E_{a} and $\tilde{A}$ of the 1,2-hydrogen shift reaction for each single event, as shown in eqs 4, 5, and 6 according to the labeling in Figure 4. E_{a} and $\tilde{A}$ are calculated on the basis of deviations from a reference reaction. The deviations are categorized as those due to the two silicon atoms central to the

TABLE 3: Single Event Arrhenius Parameters, Zero Point Energy Corrected Barriers, and Standard Enthalpies of Reaction for the First Barrier[a]

	silylene to intermediate				intermediate to silylene		
reaction	E_0, kcal mol^{-1}	log $\tilde{A}$	E_{a}, kcal mol^{-1}	$\Delta H_{\mathrm{rxn}}{}^{298}$, kcal mol^{-1}	E_0, kcal mol^{-1}	log $\tilde{A}$	E_{a}, kcal mol^{-1}
1	1.5	11.9	1.4	−0.1	1.1	13.1	1.6
2	2.3	12.1	2.3	0.9	1.0	13.1	1.5
3	2.8	12.2	2.9	1.4	1.0	13.0	1.5
4	0.7	12.3	0.7	−0.5	0.9	13.1	1.3
5	2.5	11.9	2.6	1.1	1.1	13.0	1.5
6	1.4	12.1	1.6	0.3	0.9	12.9	1.3
7	21.4	13.6	22.2	19.7	1.8	12.9	2.4
8	6.6	12.9	7.1	4.9	1.7	13.0	2.3
9	3.5	11.4	3.6	1.7	1.5	13.0	2.0
10	4.9	12.2	5.1	3.6	1.1	12.8	1.6
11	5.5	12.7	5.7	2.2	3.1	13.2	3.6
12	0.7	13.2	1.0	−2.0	2.5	13.6	3.1
13	−0.5	12.5	−0.4	−1.7	0.9	12.9	1.3
14	4.1	12.6	4.4	2.9	1.1	13.0	1.5
15	4.0	13.0	4.3	0.3	3.5	13.0	4.1
16	2.4	13.0	2.8	−0.5	2.7	13.3	3.3
17	−0.6	12.1	−0.5	−1.9	1.1	12.8	1.5
18	4.5	12.7	4.9	3.3	1.1	13.0	1.5
19	23.8	13.8	24.7	21.8	2.2	12.9	2.8
20	0.3	12.6	0.5	−1.2	1.3	13.0	1.7
21	X	X	X	X	X	X	X
22	3.6	11.6	3.9	2.8	0.7	12.7	1.0
23	3.0	11.4	3.2	2.8	0.1	12.4	0.3
24	X	X	X	X	X	X	X
25	21.2	14.2	22.0	20.6	0.9	12.7	1.3
26	2.6	12.5	3.0	0.7	1.9	12.9	2.3
27	6.9	12.6	7.2	2.8	3.9	13.3	4.6
28	3.3	12.4	3.5	3.1	0.0	12.7	0.4
29	2.2	12.2	2.3	0.7	1.2	13.1	1.6
30	1.4	12.1	1.6	0.1	1.1	13.0	1.5
31	23.0	13.5	23.7	20.5	2.7	12.9	3.3
32	1.2	11.6	1.2	−0.3	1.1	12.9	1.6
33	2.6	12.3	2.7	0.9	1.4	13.4	1.9
34	3.2	12.2	3.4	2.7	0.3	12.8	0.7
35	2.8	11.7	2.9	2.5	0.2	12.5	0.4

[a] The X indicates that the path was not mapped completely. $\tilde{A}$ has units of s^{-1}.

reaction and primary (X, Y) and secondary (N, M) contributions, where secondary contributions are grouped together as next-nearest neighbors (NNN).

$$E_a = E_a^{ref} + \sum_{i=1}^{2} \Delta GAV_{E_a}{}^0(Si_i) + \sum_{i=1}^{2} \Delta GAV_{E_a}{}^0(X_i) + \Delta GAV_{E_a}{}^0(Y_1) + \sum_j \Delta NNN_{E_a j}{}^0 \quad (4)$$

$$\log(\tilde{A}) = \log^{ref}(\tilde{A}) + \sum_{i=1}^{2} \Delta GAV_{\log(\tilde{A})}{}^0(Si_i) + \sum_{i=1}^{2} \Delta GAV_{\log(\tilde{A})}{}^0(X_i) + \Delta GAV_{\log(\tilde{A})}{}^0(Y_1) + \sum_j \Delta NNN_{\log(\tilde{A})j}{}^0 \quad (5)$$

where ΔGAV^0 is defined in eq 6:

$$\Delta GAV^0 = GAV(TS) - GAV(reactants) - GAV(reference) \quad (6)$$

The use of a reference reaction allows E_a and $\tilde{A}$ to be captured as structural deviations. Moreover, TSGA prediction accuracy can be improved easily in the future by recalculating E_a and $\tilde{A}$ for only the reference reaction, and most of the temperature dependence of the Arrhenius parameters is accounted for by the reference reaction, whereas the group additivity values are largely temperature independent. This approach also reduces the combinatorial explosion that plagues previous approaches using supergroups when more structurally diverse reactants are included. The silylsilylene−disilene isomerization was chosen as the reference reaction because it is the simplest reaction in the class, and the structure of the reactive center does not deviate considerably from the other reactions in the training set.

A more simplified formulation of TSGA was also explored. As shown in eqs 7 and 8, it was possible to include only primary contributions. This approximation was used successfully in hydrocarbon chemistry.[38−40]

$$E_a = E_a^{ref} + \sum_{i=1}^{2} \Delta GAV_{E_a}{}^0(Si_i) \quad (7)$$

$$\log(\tilde{A}) = \log^{ref}(\tilde{A}) + \sum_{i=1}^{2} \Delta GAV_{\log(\tilde{A})}{}^0(Si_i) \quad (8)$$

The primary silicon atoms were differentiated according to the number of Si and H atoms to which they were attached. The five primary contributions to the reactive center used in TSGA were (1) $Si_1-(H)_3$, (2) $Si_1-(Si)(H)_2$, (3) $Si_1-(Si)_2(H)$, (4) $Si_2-(H)$, and (5) $Si_2-(Si)$. When the reactive centers were part of a ring (endocyclic) or adjacent to a ring (exocyclic),

TABLE 4: Single Event Arrhenius Parameters, Zero Point Energy Corrected Barriers, and Standard Enthalpies of Reaction for the Second Barrier[a]

	intermediate to silene				silene to intermediate		
reaction	E_0, kcal mol^{-1}	log $\tilde{A}$	E_a, kcal mol^{-1}	$\Delta H_{rxn}{}^{298}$, kcal mol^{-1}	E_0, kcal mol^{-1}	log $\tilde{A}$	E_a, kcal mol^{-1}
1	6.7	13.3	7.2	−7.2	14.1	12.9	14.2
2	6.8	13.3	7.3	−9.9	16.9	12.9	17.1
3	7.1	13.3	7.6	−11.8	19.1	12.9	19.4
4	4.9	13.5	5.3	−8.3	13.4	13.0	13.5
5	4.6	13.3	5.0	−13.3	18.0	12.5	18.4
6	4.9	13.4	5.2	−11.0	16.0	12.9	16.2
7	6.4	13.7	7.1	−13.4	19.8	13.7	20.5
8	6.5	13.3	7.0	−11.6	18.1	13.2	18.6
9	6.9	13.3	7.4	−11.8	18.8	13.1	19.2
10	6.4	13.2	6.9	−12.2	18.7	13.1	19.1
11	5.9	13.5	6.8	−1.4	7.5	13.1	8.0
12	7.9	13.4	8.5	−10.7	18.6	13.1	19.2
13	6.3	13.3	6.8	−9.5	16.0	12.5	16.3
14	4.5	13.2	4.9	−11.6	16.3	13.0	16.5
15	5.8	13.5	6.6	−1.9	7.9	12.8	8.4
16	7.6	13.3	8.2	−12.9	20.5	13.2	21.1
17	6.1	13.1	6.6	−11.9	18.1	12.6	18.6
18	4.6	13.2	5.0	−14.1	18.7	13.0	19.2
19	5.9	13.5	6.5	−12.5	18.5	13.6	19.0
20	7.5	13.3	8.1	−12.5	20.1	13.1	20.7
21	X	X	X	X	X	X	X
22	4.8	12.9	5.1	−12.3	17.1	12.3	17.5
23	4.2	12.4	4.4	−12.9	17.0	12.4	17.4
24	X	X	X	X	X	X	X
25	4.8	13.7	5.3	−12.6	17.4	13.8	18.1
26	3.4	13.0	3.8	−12.3	15.9	12.0	16.2
27	2.3	13.2	2.9	0.8	1.7	12.7	2.0
28	2.7	12.8	3.1	−11.8	14.6	12.3	14.9
29	6.8	13.4	7.3	−9.9	16.9	13.1	17.2
30	4.9	13.4	5.3	−10.7	15.9	12.7	16.1
31	5.1	13.5	5.7	−11.5	16.8	13.4	17.2
32	6.7	13.3	7.3	−9.0	16.0	13.1	16.2
33	6.8	13.5	7.4	−11.1	18.2	12.5	18.5
34	4.2	13.2	4.5	−13.2	17.5	12.7	17.8
35	4.5	13.0	4.7	−10.6	15.1	12.5	15.3

[a] The X indicates that the path was not mapped completely. $\tilde{A}$ has units of s^{-1}.

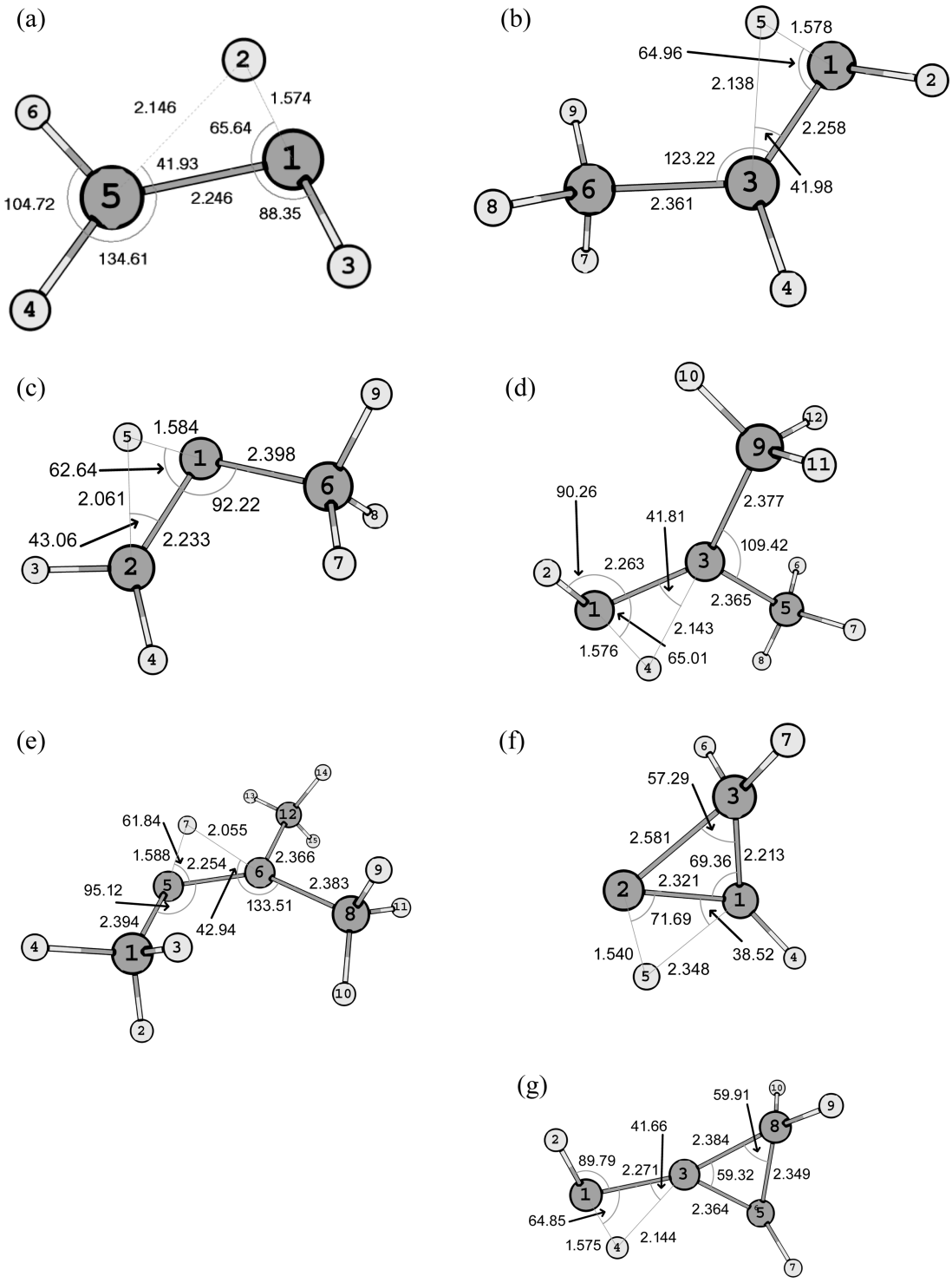

Figure 5. B3LYP/6-31G(d) optimized geometries of the lowest energy conformer of the second transition state for key reactions: (a) no silyl groups, (b) one silyl group on Si_1, (c) one silyl group on Si_2, (d) two silyl groups on Si_1, (e) two silyl groups on Si_1 and one on Si_2, (f) endocyclic isomerization for three-membered ring, and (g) exocyclic isomerization for three-membered ring. Si_1 and Si_2 notation corresponds to that in Figure 4. Part (a) is the reference reaction.

additional terms were included to account for structural deviations. When a molecule contained a single ring, inclusion of ring corrections was straightforward. However, when multiple rings were present for a given silicon hydride, two rules were followed: (1) in the case of fused polycyclic systems, the ring contribution nearest to the reactive center (exo- or endocyclic) was used, and (2) in molecules with two nonfused rings about the reactive center, the smaller ring correction was used because the effect on the reactive center for the more sterically strained ring dominates the structural changes of the silicon hydride. For example, in Table 2, the polycyclic species in reaction 27 (bicyclo-[3.1.0]hexa-6-silylene to bicyclo[3.1.0]hexa-6-silene) was assigned only one endocyclic three-membered ring correction, and the two nonfused rings in reactions 24 and 25 were assigned only one exocyclic, three-membered ring correction. This strategy reduces the number of parameters needed in estimation of E_a and $\tilde{A}$ while still capturing the data accurately.

TABLE 5: (a) TSGA Parameters for Prediction of E_a at Different Levels of Statistical Significance; (b) Statistical Analysis for Least Squares Regression of E_a TSGA Parameters

E_a (kcal mol^{-1})												
					ring size							
(a)		primary contributions			endocyclic silylene				exocyclic silylene			
reaction	parameter t-test α-level	$Si_1-(Si)(H)_2$	$Si_1-(Si)_2H$	$Si_2-(Si)$	3	4	5	6	3	4	5	6
silylene to silene	full	1.4	1.5	−2.5	1.9	1.1	−1.1	2.1	18.4	3.4	0.6	1.9
	α = 0.1	1.5	1.7	−2.6	1.9	X	X	2.1	18.2	3.2	X	1.8
	α = 0.05	2.2	2.7	−2.7	X	X	X	X	17.2	X	X	X
silene to silylene	Full	3.0	4.9	−0.9	−9.1	2.8	0.1	0.5	1.4	−0.5	0.1	−0.1
	α = 0.1	3.0	4.9	−0.6	−9.3	2.6	X	X	1.4	X	X	X
	α = 0.05	3.0	4.9	−0.6	−9.3	2.6	X	X	1.4	X	X	X

		E_a		
			regression F-test	
(b)				
reaction	parameter t-test α-level	R^2-value	F-value	P-value
silylene to silene	full	0.992	68	<0.001
	α = 0.1	0.981	59	<0.001
	α = 0.05	0.943	54	<0.001
silene to silylene	full	0.996	123	<0.001
	α = 0.1	0.994	299	<0.001
	α = 0.05	0.994	299	<0.001

TABLE 6: (a) TSGA Parameters for Prediction of Log $\tilde{A}$ at Different Levels of Statistical Significance. $\tilde{A}$ has Units of s^{-1}; (b) Statistical Analysis for Least Squares Regression of Log $\tilde{A}$ TSGA Parameters

Log $\tilde{A}$												
					ring size							
(a)		primary contributions			endocyclic silylene				exocyclic silylene			
reaction	parameter t-test α-level	Si_1-$(Si)(H)_2$	Si_1-$(Si)_2H$	Si_2-(Si)	3	4	5	6	3	4	5	6
silylene to silene	full	0.20	0.21	0.34	0.69	0.45	0.09	0.31	2.15	0.98	−0.48	0.40
	α = 0.1	X	X	0.71	0.53	X	X	X	2.36	1.19	X	X
	α = 0.05	X	X	0.80	X	X	X	X	2.36	1.19	X	X
silene to silylene	full	−0.02	−0.11	−0.05	0.15	0.34	−0.24	0.22	0.94	0.41	0.34	0.31
	α = 0.1	X	X	X	X	X	X	X	0.83	X	X	X
	α = 0.05	X	X	X	X	X	X	X	0.83	X	X	X

		Log $\tilde{A}$		
			regression F-test	
(b)				
reaction	parameter t-test α-level	R^2-value	F-value	P-value
silylene to silene	full	0.968	17	0.001
	α = 0.1	0.910	33	<0.001
	α = 0.05	0.882	35	<0.001
silene to silylene	full	0.882	4	0.048
	α = 0.1	0.464	14	0.002
	α = 0.05	0.464	14	0.002

To develop the TSGA parameters, the training set shown in Table 1 was used. The reactions are shown using notation typically used for hydrocarbons, but each multivalent atom depicted is a silicon atom, which contains the identical number of valence electrons as carbon. The silicon hydrides in the training set had a maximum of seven silicon atoms. In Table 1, reactions 1−6 explore all possible acyclic primary contributions to the reactive center. Reactions 7−10 explore exocyclic ring contributions where the 1,2-hydrogen shift occurs adjacent to a ring. Reactions 11−18 explore endocyclic ring contributions (i.e., the 1,2-hydrogen shift occurs in a ring). Rings larger than six silicon atoms were not examined because (1) larger systems are computationally more intensive for quantum chemical calculations and (2) polycrystalline silicon without defects will assume a diamond cubic structure where six-membered rings form a series of hexagonal channels, and larger ring sizes are thermodynamically unfavored.[55]

The TSGA parameters were obtained using multiple linear regression with the least-squares method for all training set reactions. The overall model was deemed significant if the F-test satisfied the 95% confidence level (i.e., the p-value was below α = 0.05). The significance of each TSGA parameter of the model was then determined with a t-test at the 90% and 95% confidence levels. All insignificant parameters were removed from the model. Four 11-parameter databases were obtained from 18 training set reactions: one each for E_a and log $\tilde{A}$ of the forward and reverse steps of 1,2-hydrogen shift. The TSGA parameter databases were then validated against 17 reactions that were not included in the training set. These validation set reactions are displayed in Table 2. The molecules comprising

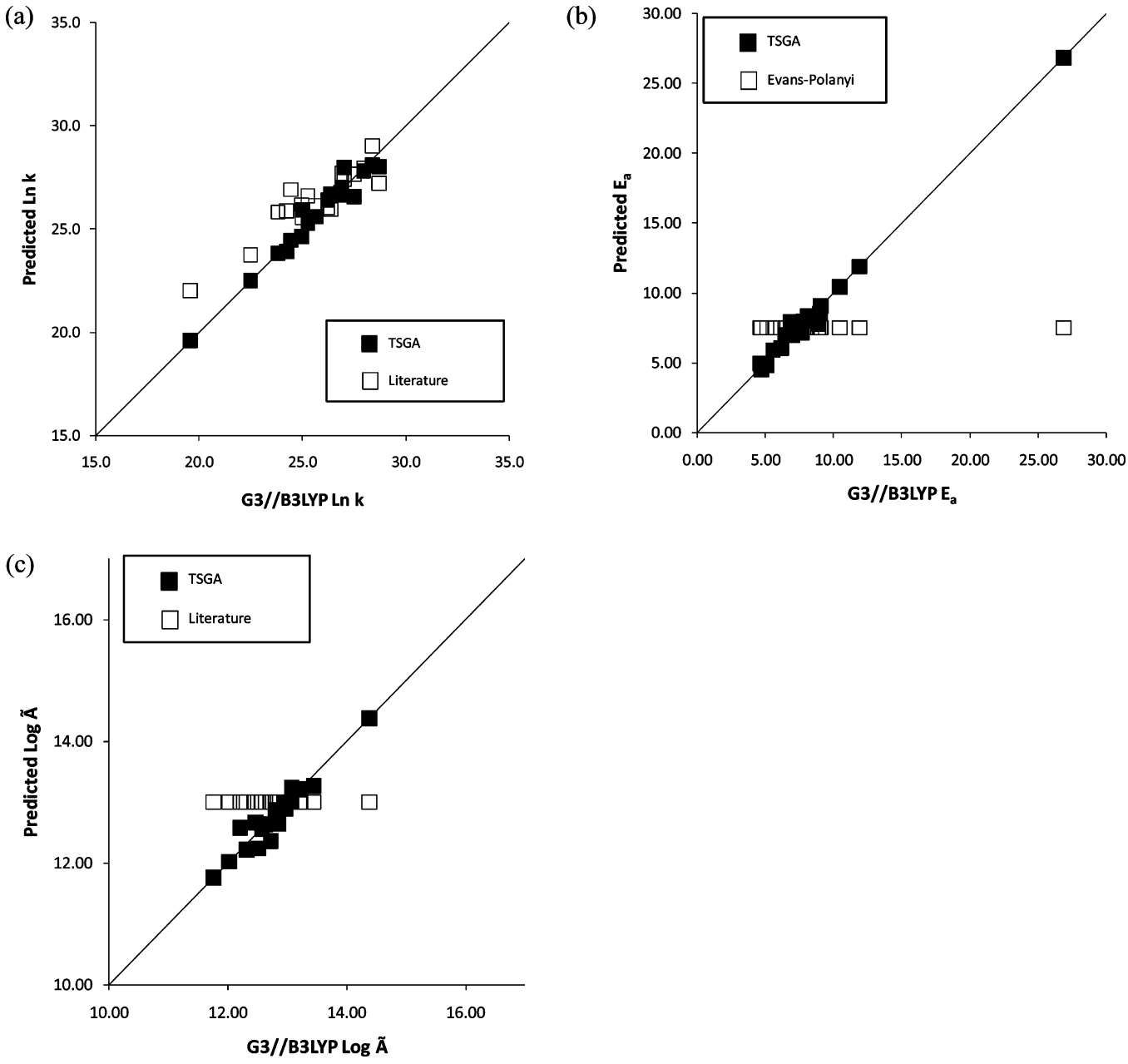

Figure 6. Parity plots of substituted silylene to silene isomerization for training reactions at 1000 K and 1 atm: (a) ln k (units for k are s^{-1}), (b) E_a (units are kcal mol^{-1}), (c) log $\tilde{A}$ (units for $\tilde{A}$ are s^{-1}).

the validation set reactions are either polycyclic, contain multiple nonfused rings, or explore large silicon hydrides containing up to 10 silicon atoms.

Finally, the results of TSGA were compared with the prediction of E_a and $\tilde{A}$ from the literature, which are based on a representative value ($\tilde{A} = 1 \times 10^{13}$ s^{-1})[1] and the Evans−Polanyi correlation ($E_a = E_0 + \gamma\ \Delta H_{Rxn}$; $E_0 = 7.5$ kcal mol^{-1}; $\gamma = 0$ for substituted silylene to silene isomerization; $\gamma = 1$ for silene to substituted silylene isomerization).[3,15]

Results and Discussion

Presence of Two Barriers. A total of 35 1,2-hydrogen shift reactions were mapped using G3//B3LYP. Mapping of the 1,2-hydrogen shift potential energy surface for all but two of the reactions showed two distinct barriers linked by a common intermediate, which is a stable 1,2-bridged species as depicted in Figure 1 for silylsilylene-disilene isomerization. Interestingly, the intermediate is not present at the HF/6-31G(d) level, but when electron correlation is included (e.g., MP2/6-31G(d)), the 1,2-bridged intermediate is stabilized. Passage through a stable intermediate by way of two barriers in series corroborates the experimental work of McCarthy et al.[18] As opposed to the 1,2-hydrogen shift reaction in carbenes,[56] 1,2-hydrogen bridging in silicon hydrides is possible due to the larger molecular orbitals present in the silicon atom. A summary of the zero-point corrected energy barriers, the regressed $\tilde{A}$ and E_a values, and the standard enthalpies of reaction for the formation of the intermediate from a substituted silylene are summarized in Table 3. The same information is tabulated in Table 4 for the conversion of the 1,2-bridged intermediate to the silene. Intrinsic reaction coordinate following shows the absence of a stable intermediate for reactions 21 and 24. Wiberg bond

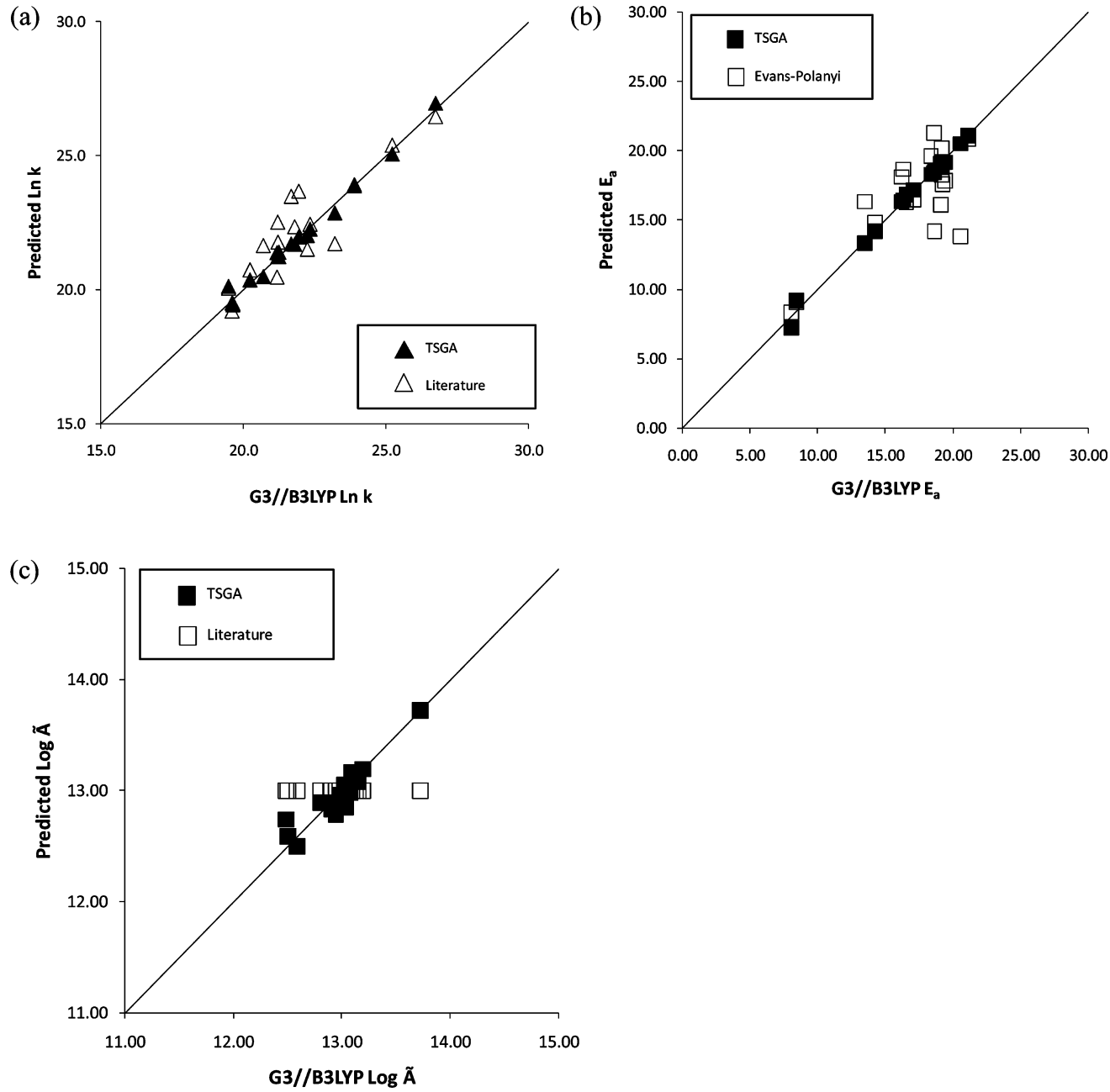

Figure 7. Parity plots of silene to substituted silylene isomerization for training reactions at 1000 K and 1 atm: (a) ln k (units for k are s^{-1}), (b) E_a (units are kcal mol^{-1}), (c) log $\tilde{A}$ (units for $\tilde{A}$ are s^{-1}).

index calculations[57] show stronger dative bond formation closest to a small ring substituent that stabilizes the divalent center for these reactions.[48]

The formation of the stable intermediate from the substituted silylene is nearly always endothermic. The Hammond postulate predicts a late transition state, that is, one that resembles the product, and this is borne out by the fact that the transition state for the first barrier resembles the stable intermediate. The standard enthalpies of reaction were mildly exothermic for reactions in which the divalent silicon atom was part of a four- or five-membered ring. The heat of reaction never exceeds 5 kcal mol^{-1}, except when the substituted silylene has a three-membered ring substitution. The presence of a three-membered ring substituent induces standard enthalpies of reaction that range from 20 to 22 kcal mol^{-1}. The associated barriers are also high, indicating that the formation of an exocyclic π bond is not favored, as compared to formation of a four-membered ring from these substituted silylenes. The formation of intermediates from divalent silicon atoms in a five-membered ring was found to have very small apparent negative activation energies.

The transformation of the intermediate to a silene is highly exothermic, revealing that the intermediate is enthalpically uphill from both the substituted silylene and the silene. The transition state for the second barrier also resembles the stable intermediate because in this case, it is an early transition state in the forward direction. All the standard enthalpies of reaction are negative except for the formation of the π bond of bicyclo[3.1.0]hexa-6-silene in reaction 27, where the polycyclic nature of the reactive center restricts the formation of a nonplanar *trans*-silene. Reaction 18 displays the highest exothermicity, where an endocyclic π bond in a six-membered ring is highly favorable because the steric hindrance associated with substituents across the reactive center is minimized.

TABLE 7: Ratio of $k^{G3//B3LYP}$ and k^{TSGA} of the Training Set for the Substituted Silylene to Silene Isomerization Using the Full Parameter Model

	ratio of k^{TSGA} and $k^{G3//B3LYP}$			
	temperature (K)			
reaction	298	750	1000	1200
1	1.00	1.00	1.00	1.00
2	0.50	0.67	0.70	0.72
3	1.26	0.76	0.70	0.67
4	0.63	0.51	0.49	0.48
5	2.90	2.56	2.51	2.49
6	0.54	0.77	0.82	0.84
7	1.00	1.00	1.00	1.00
8	1.00	1.00	1.00	1.00
9	1.00	1.00	1.00	1.00
10	1.00	1.00	1.00	1.00
11	9.21	3.09	2.58	2.36
12	0.45	0.78	0.86	0.90
13	1.07	0.78	0.74	0.72
14	0.83	1.04	1.07	1.09
15	0.11	0.32	0.39	0.42
16	2.24	1.28	1.17	1.12
17	0.94	1.28	1.35	1.39
18	1.20	0.97	0.93	0.92

TABLE 8: Ratio of $k^{G3//B3LYP}$ and k^{TSGA} of the Training Set for the Silene to Substituted Silylene Isomerization Using the Full Parameter Model

	ratio of k^{TSGA} and $k^{G3//B3LYP}$			
	temperature (K)			
reaction	298	750	1000	1200
1	1.00	1.00	1.00	1.00
2	0.74	0.85	0.87	0.88
3	1.07	0.82	0.79	0.77
4	0.79	0.70	0.69	0.68
5	1.98	1.87	1.86	1.85
6	0.64	0.76	0.78	0.79
7	1.00	1.00	1.00	1.00
8	1.00	1.00	1.00	1.00
9	1.00	1.00	1.00	1.00
10	1.00	1.00	1.00	1.00
11	3.04	1.37	1.21	1.13
12	1.19	1.19	1.19	1.19
13	0.96	1.11	1.14	1.15
14	0.61	0.85	0.90	0.93
15	0.33	0.73	0.83	0.89
16	0.84	0.84	0.84	0.84
17	1.04	0.90	0.88	0.87
18	1.63	1.17	1.11	1.08

Figure 5 shows the transition state geometries for the transformation of the intermediate to a silene for several key reactions. The structural changes upon addition of various substituents to either side of the reactive center can be seen by comparing these geometries. Similar to the singlet carbenes of hydrocarbon chemistry, the presence of an sp^2-hybridized divalent silicon center strains the angle made by the two central substituents. Endocyclic substituted silylenes reduce the central bond angle even lower due to additional ring strain across the reactive center (Figure 5f). Acyclic substituents do not change the reactive center greatly (Figures 5a−d); however, when all three substituents are a silyl group, the steric hindrance of these groups plays a role in the 1,2-hydrogen shift reaction (Figure 5e). Exocyclic substituted silylenes introduce ring strain as well (Figure 5g), but only on the donor silicon atom (i.e., the silicon atom from which the migrating hydrogen atom is leaving), which stabilizes the divalent silicon atom.[48] The structure of the reactive center changes the most with the addition of small rings across or adjacent to the hydrogen migration.

TABLE 9: Ratio of $k^{G3//B3LYP}$ and k^{TSGA} of the Validation Set for the Substituted Silylene to Silene Isomerization Using the Full Parameter Model

	ratio of k^{TSGA} and $k^{G3//B3LYP}$		
	temperature (K)		
reaction	750	1000	1200
19	2.47	1.90	1.67
20	1.32	1.36	1.38
21	1.40	0.95	0.78
22	4.19	3.33	2.96
23	27.43	22.23	20.02
24	2.45	2.54	2.58
25	1.05	0.80	0.70
26	0.28	0.37	0.42
27	1.44	2.13	2.60
28	0.74	1.02	1.21
29	0.35	0.38	0.39
30	0.82	0.89	0.92
31	1.31	1.48	1.56
32	0.57	0.72	0.82
33	0.51	0.55	0.56
34	2.12	1.71	1.54
35	5.26	4.22	3.78

TABLE 10: Ratio of $k^{G3//B3LYP}$ and k^{TSGA} of the Validation Set for the Silene to Substituted Silylene Isomerization Using the Full Parameter Model

	ratio of k^{TSGA} and $k^{G3//B3LYP}$		
	temperature (K)		
reaction	750	1000	1200
19	0.48	0.62	0.70
20	0.72	0.78	0.81
21	2.84	3.26	3.50
22	3.31	3.86	4.16
23	1.29	1.49	1.61
24	0.94	1.59	2.08
25	0.26	0.34	0.39
26	1.30	1.86	2.23
27	0.01	0.04	0.08
28	0.29	0.57	0.80
29	0.55	0.55	0.56
30	1.24	1.30	1.33
31	0.22	0.38	0.51
32	0.33	0.39	0.42
33	1.10	1.24	1.31
34	0.71	0.78	0.81
35	1.12	1.35	1.47

While our calculations reveal that the 1,2-bridged intermediate is clearly stable, it is unwieldy to have to track it explicitly in mechanistic models because schemes for predicting the properties of these intermediates are not available. It is more convenient to consolidate the two-step conversion of a substituted silylene to a silene and its reverse reaction into one overall transformation. All of the combined reactions are exothermic except for reactions containing silylenes substituted with a three-membered ring and endocyclic substituted silylenes of polycyclic nature or only three silicon atoms. The 1,2-hydrogen shift reaction to form a silene is not favored for these silicon hydrides. Prior to consolidation of the two-step conversion, the rate-limiting step was first validated by monitoring the reaction dynamics of an unfavored and a favored silene formation (i.e., reactions 7 and 18, respectively). Three microkinetic models were created assuming (1) a full model, (2) that the second step is rate-limiting, and (3) that the first step is rate-limiting. Model

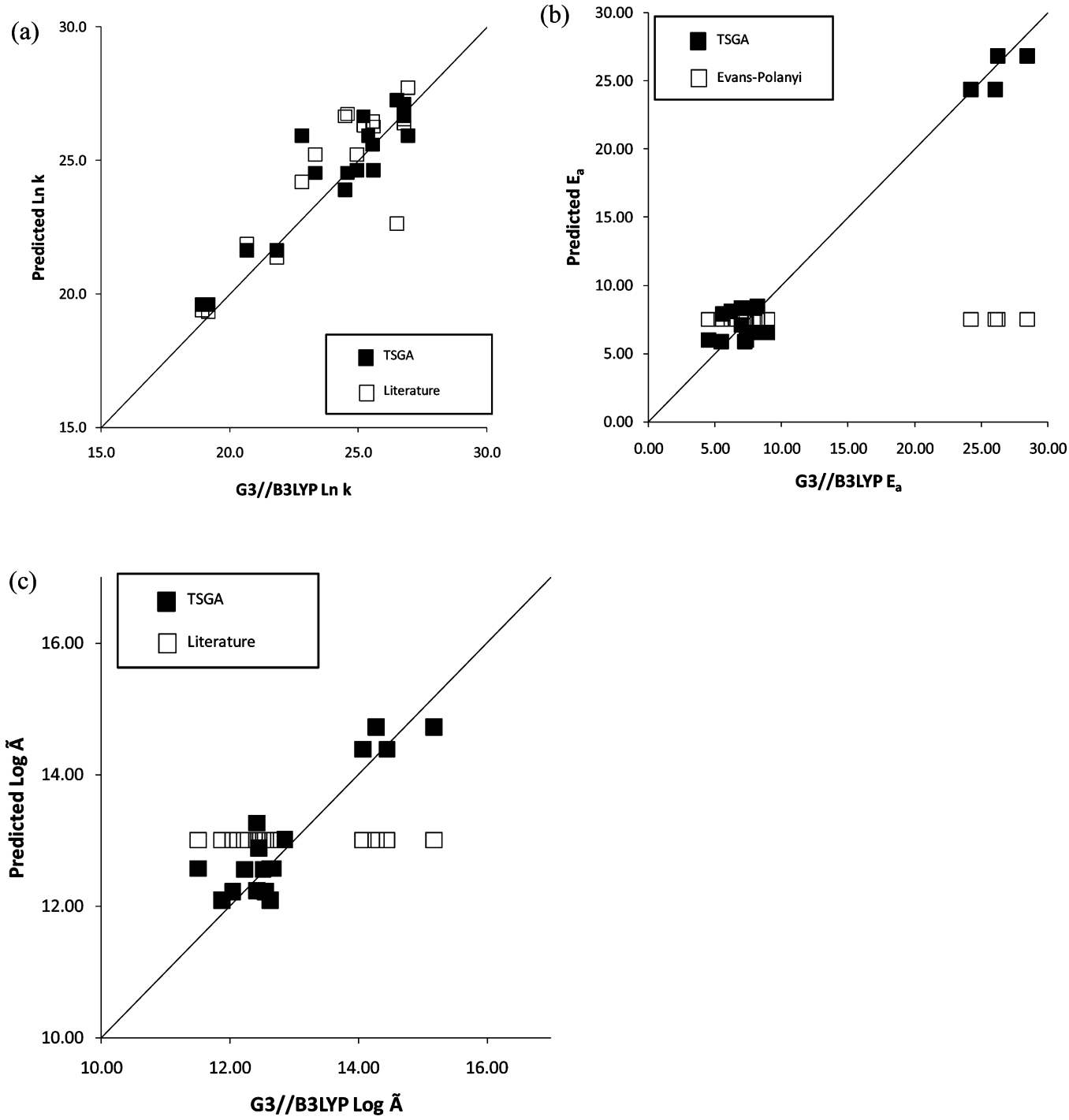

Figure 8. Parity plots of substituted silylene to silene isomerization for validation reactions at 1000 K and 1 atm: (a) ln k (units for k are s^{-1}), (b) E_a (units are kcal mol^{-1}), (c) log $\tilde{A}$ (units for $\tilde{A}$ are s^{-1}).

1 explicitly includes the kinetic parameters for both reaction steps without assuming a rate-limiting step. The overall rate coefficient for model 2 was calculated as $k = K_1k_2$, where K_1 is the equilibrium coefficient for the first step and k_2 is the rate coefficient for the second step. Model 3 calculates the overall rate coefficient as $k = k_1$, where k_1 is the rate coefficient for the first step. Over the temperature range of 750−1200 K, model 2 is superior in predicting the reaction dynamics of the full model for both reactions 7 and 18. When the temperature is above 1385 K, model 3 marginally outperforms model 2 for reaction 7. Thus, the 1,2-hydrogen shift reaction was assumed to be rate-limited by the second step over the temperature range of this study. A summary of the zero-point corrected energy barriers, the regressed E_a and $\tilde{A}$ values, the standard enthalpies of reaction, and reaction path degeneracies for the formation of the silene from a substituted silylene are summarized in the Supporting Information.

TSGA Parameters. TSGA parameters were regressed from the training set reactions of Table 1. The matrices used to derive the TSGA parameters were constructed using a sum of the primary contributions and the presence/absence of an endocyclic or exocyclic ring correction. Table 5 summarizes the results of various least-squares regressions for E_a, and Table 6 summarizes the same information for log $\tilde{A}$. The full parameter model contains 11 parameters. The TSGA group values for the full model are summarized in Tables 5a and 6a for E_a and $\tilde{A}$,

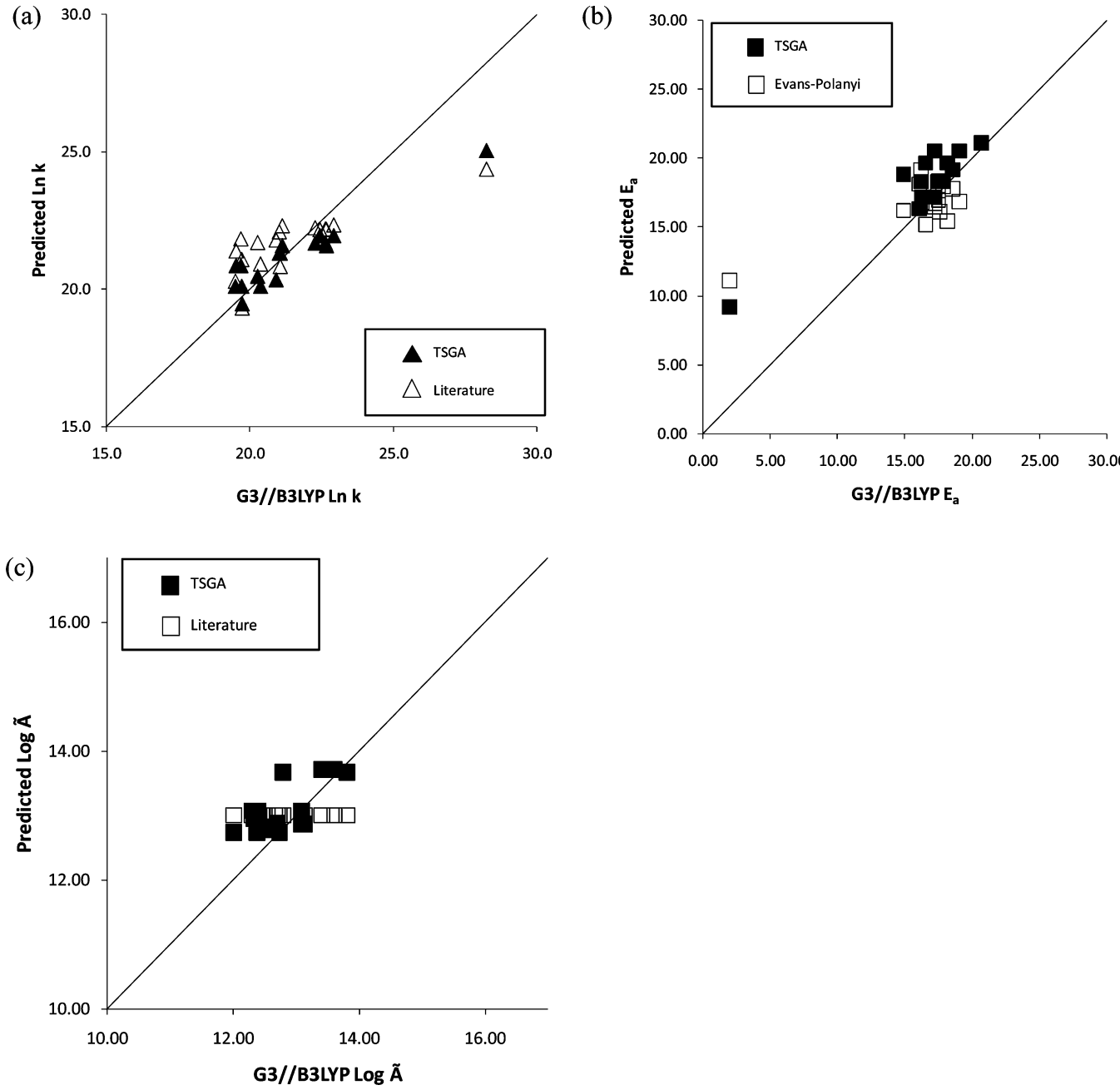

Figure 9. Parity plots of silene to substituted silylene isomerization for validation reactions at 1000 K and 1 atm: (a) ln k (units for k are s^{-1}), (b) E_a (units are kcal mol^{-1}), (c) log $\tilde{A}$ (units for $\tilde{A}$ are s^{-1}).

respectively. Parity plots depicting how well the full model captures the training set values of k, E_a, and $\tilde{A}$ at 1000 K for substituted silylene to silene isomerization and silene to substituted silylene isomerization are shown in Figures 6a−c and 7a−c, respectively. The values predicted by the kinetic correlation in the literature are also provided for comparison. It is clear from these plots that the ability of TSGA to capture the k values at 1000 K is only slightly superior to that of the literature correlations. However, the ability of TSGA to capture E_a and $\tilde{A}$ is clearly superior. A performance summary for the 1,2-hydrogen shift reaction for these reactions is provided in Tables 7 and 8 for substituted silylene to silene and silene to substituted silylene isomerizations, respectively. The G3//B3LYP and TSGA rate coefficients for all training set reactions can be found in the Supporting Information.

Two additional models were explored on the basis of eliminating parameters from the full model that did not meet the t-test statistic at the (1) 95% and (2) 90% confidence levels for $\tilde{A}$ and E_a separately. According to the F-test, all of the regressed models were statistically significant at the 95% confidence level. The statistics for these two models are summarized in Tables 5b and 6b for E_a and $\tilde{A}$, respectively. The TSGA parameters for E_a are summarized in Table 5a, and log $\tilde{A}$ values are summarized in Table 6a. For the prediction of E_a using TSGA, corrections for endocyclic and exocyclic substituted silylenes of three-, four-, and six-membered rings as well as all primary contributions are statistically significant at the 90% confidence level. For the prediction of log $\tilde{A}$ using TSGA, only parameters pertaining to exocyclic three- and four-membered rings, three-membered endocyclic rings, and one primary contribution are necessary for a statistically significant model at the 90% confidence level. The number of parameters is reduced further for $\tilde{A}$ and E_a at the 95% confidence level.

However, as summarized in Tables 5b and 6b, the goodness of fit is decreased in both cases as compared to the full parameter model.

These more simplified models reveal that the reference reaction captures the single event pre-exponential factor, $\tilde{A}$, for the 1,2-hydrogen shift reaction relatively well and pinpoint the more significant structural factors affecting the $\tilde{A}$ value. In the transformation of a substituted silylene to a silene, the most significant deviations from the reference reaction arise when substituted silylenes have substituents consisting of three- and four-membered rings or when a silicon atom is added adjacent to the divalent silicon atom. The transformation of a silene to a substituted silylene is captured well by the reference reaction, except when the substituted silylene has a three-membered ring substituent. When any of these deviations from the reference reaction is present, the pre-exponential factor increases as compared to the value of the reference reaction.

These analyses also reveal that the E_a values for substituted silylenes undergoing the 1,2-hydrogen shift reaction are not captured very well by the reference reaction alone. All three TSGA parameters pertaining to the primary contributions to the reactive center remain statistically significant at the 95% confidence level. When transforming a substituted silylene to a silene, addition of silicon atoms to the donor silicon atom always increases E_a. In contrast, addition of a silicon atom adjacent to the divalent center decreases E_a. Silylenes substituted with a three-membered ring have an increased E_a value compared to the reference reaction. In the reverse direction, the primary contributions and exocyclic substituted silylenes affect E_a in the same way as for the forward direction; however, endocyclic substituted silylenes of three- and four-membered rings decrease and increase E_a, respectively.

Validation of TSGA Parameters. The TSGA parameters were then tested by comparing the predictions from the TSGA method against the G3//B3LYP values for the validation reactions in Table 2. A performance summary for the 1,2-hydrogen shift reaction for these reactions is provided in Tables 9 and 10 for substituted silylene to silene and silene to substituted silylene isomerizations, respectively. The G3//B3LYP and TSGA rate coefficients for all validation set reactions can be found in the Supporting Information. For 15 validation set reactions in the temperature range of 750−1200 K, the TSGA and G3//B3LYP rate coefficients were within an average factor of 2. Reactions 23 and 27 deviated more significantly in the substituted silylene to silene and silene to substituted silylene directions, respectively, but the predictions were still within a factor of 25 at 1000 K.

It is interesting to examine how well the 1,2-hydrogen shift reaction for polycyclic species is predicted by TSGA. For systems containing large rings (e.g., reaction 28), the prediction is very good. However, reactions involving polycyclics composed of smaller rings (e.g., reaction 27) are predicted less well; a π bond is not favored, and TSGA underpredicts the rate coefficient for the transformation of the silene to a substituted silylene. Acyclic species with tertiary silicon atoms (e.g., reaction 23) that sterically hinder the reactive center are also not captured as well by TSGA; the rate coefficient for transformation of the substituted silylene to a silene is overpredicted.

Finally, the predictions of TSGA were compared with those of the literature correlations for the reactions comprising the validation set. Parity plots of the rate coefficients at 1000 K and 1 atm, E_a, and $\tilde{A}$ for both TSGA and the literature correlations are provided in Figures 8a−c and 9a−c. The sum of squared errors between the rate coefficients predicted by TSGA and the G3//B3LYP values is lower than that for the literature correlations. However, the superiority of TSGA is even more clearly demonstrated when the $\tilde{A}$ and E_a values are examined individually. Thus, the predictive capability of TSGA over a wide range of $\tilde{A}$ and E_a is preferred in the calculation of rate coefficients for the 1,2-hydrogen shift reaction.

Conclusions

Rate coefficients and Arrhenius parameters for the 1,2-hydrogen shift reaction have been calculated for 35 reactions using G3//B3LYP, statistical thermodynamics, and conventional transition state theory. The overall reaction of a substituted silylene to silene was found to pass through a stable intermediate that decomposes via an exothermic reaction for nearly all silicon hydrides. The kinetic parameters for the two elementary steps were calculated separately, the rate-determining step was determined to be from the intermediate to the silene, and then kinetic parameters for the overall reaction were calculated to align better with mechanistic modeling efforts.

A group additivity model has been extended to single event pre-exponential factors, $\tilde{A}$, and activation energies, E_a, for the 1,2-hydrogen shift reactions of silicon hydrides. The 1,2-hydrogen shift reaction was explored for acyclic, cyclic, and polycyclic monofunctional silicon hydrides, and the structural moieties around the reactive center that have the most dominant influence on the kinetic parameters were identified. The TSGA method outperforms the methods in the literature that are currently used to estimate Arrhenius parameters for this class of reactions. The mean absolute ratio of predicted rate coefficients for a validation set of 17 reactions was lower for TSGA than for current literature methods to predict rate coefficients for 1,2-hydrogen shift.

Acknowledgment. We are grateful for the support of this work by the following organizations: (1) National Science Foundation ([a] Collaborative Research Grant CBET-0500320: International Research and Education in Engineering; [b] NCSA Teragrid Supercomputing Facilities), (2) Laboratory for Chemical Technology at the Ghent University in Belgium by way of an international fellowship to Andrew J. Adamczyk, and (3) the ARCS Foundation Inc. for fellowship support of Andrew J. Adamczyk.

Supporting Information Available: Geometries and frequencies for all species (Tables S1−S35). Summary of the zero-point corrected energy barriers, the regressed E_a and $\tilde{A}$ values, the standard enthalpies of reaction, and reaction path degeneracies for the formation of the silene from a substituted silylene (Table S36). G3//B3LYP and full parameter model TSGA rate coefficients for all reactions (Table S37). This material is available free of charge via the Internet at http://pubs.acs.org.

References and Notes

(1) Swihart, M. T.; Girshick, S. L. *J. Phys. Chem. B* **1999**, *103*, 64.
(2) Dollet, A.; de Persis, S. *J. Anal. Appl. Pyrol.* **2007**, *80*, 460.
(3) Wong, H. W.; Li, X. G.; Swihart, M. T.; Broadbelt, L. J. *J. Phys. Chem. A* **2004**, *108*, 10122.
(4) Li, X. G.; He, Y. Q.; Talukdar, S. S.; Swihart, M. T. *Langmuir* **2003**, *19*, 8490.
(5) Schatz, G. C. *Proc. Natl. Acad. Sci. U.S.A.* **2007**, *104*, 6885.
(6) Swihart, M. T.; Li, X. G.; He, Y. Q.; Kirkey, W.; Cartwright, A. N.; Sahoo, Y.; Prasad, P. N. *High-rate synthesis and characterization of brightly luminescent silicon nanoparticles with applications in hybrid materials for photonics and biophotonics*; Conference on Nanocrystals and Organic and Hybrid Nanomaterials, San Diego, CA, 2003.
(7) Dolgonos, G. *Chem. Phys. Lett.* **2008**, *466*, 11.

(8) West, R.; Fink, M. J. *Science* **1981**, *214*, 1343.
(9) Ernst, M. C.; Sax, A. F.; Kalcher, J. *Chem. Phys. Lett.* **1993**, *216*, 189.
(10) Ho, P.; Coltrin, M. E.; Binkley, J. S.; Melius, C. F. *J. Phys. Chem.* **1986**, *90*, 3399.
(11) Gordon, M. S.; Truong, T. N.; Bonderson, E. K. *J. Am. Chem. Soc.* **1986**, *108*, 1421.
(12) Kroghjespersen, K. *Chem. Phys. Lett.* **1982**, *93*, 327.
(13) Katzer, G.; Ernst, M. C.; Sax, A. F.; Kalcher, J. *J. Phys. Chem. A* **1997**, *101*, 3942.
(14) Curtiss, L. A.; Raghavachari, K.; Deutsch, P. W.; Pople, J. A. *J. Chem. Phys.* **1991**, *95*, 2433.
(15) Swihart, M. T.; Carr, R. W. *J. Phys. Chem. A* **1998**, *102*, 785.
(16) White, R. T.; Espinorios, R. L.; Rogers, D. S.; Ring, M. A.; Oneal, H. E. *International Journal of Chemical Kinetics* **1985**, *17*, 1029.
(17) Maier, G.; Reisenauer, H. P.; Glatthaar, J. *Chem.—Eur. J.* **2002**, *8*, 4383.
(18) McCarthy, M. C.; Yu, Z.; Sari, L.; Schaefer, H. F.; Thaddeus, P. *J. Chem. Phys.* **2006**, *124*, 7.
(19) Weerts, W. L. M.; de Croon, M.; Marin, G. B. *J. Electrochem. Soc.* **1998**, *145*, 1318.
(20) Johannes, J. E.; Ekerdt, J. G. *J. Electrochem. Soc.* **1994**, *141*, 2135.
(21) Becerra, R.; Walsh, R. *J. Phys. Chem.* **1987**, *91*, 5765.
(22) Dickinson, A. P.; Oneal, H. E.; Ring, M. A. *Organometallics* **1991**, *10*, 3513.
(23) Ottosson, H.; Eklof, A. M. *Coord. Chem. Rev.* **2008**, *252*, 1287.
(24) Kaiser, R. I.; Osamura, Y. *Astron. Astrophys.* **2005**, *432*, 559.
(25) Broadbelt, L. J.; Stark, S. M.; Klein, M. T. *Chem. Eng. Sci.* **1994**, *49*, 4991.
(26) Broadbelt, L. J.; Stark, S. M.; Klein, M. T. *Comput. Chem. Eng.* **1996**, *20*, 113.
(27) Broadbelt, L. J.; Stark, S. M.; Klein, M. T. *Ind. Eng. Chem. Res.* **1995**, *34*, 2566.
(28) Broadbelt, L. J.; Stark, S. M.; Klein, M. T. *Ind. Eng. Chem. Res.* **1994**, *33*, 790.
(29) Klinke, D. J.; Broadbelt, L. J. *AIChE J.* **1997**, *43*, 1828.
(30) Susnow, R. G.; Dean, A. M.; Green, W. H.; Peczak, P.; Broadbelt, L. J. *J. Phys. Chem. A* **1997**, *101*, 3731.
(31) Broadbelt, L. J.; Pfaendtner, J. *AIChE J.* **2005**, *51*, 2112.
(32) Evans, M. G.; Polanyi, M. *Faraday Soc.* **1938**, *34*, 11.
(33) Benson, S. W. *Thermochemical Kinetics*, 2nd ed.; Wiley: New York, 1976.
(34) Wong, H. W.; Nieto, J. C. A.; Swihart, M. T.; Broadbelt, L. J. *J. Phys. Chem. A* **2004**, *108*, 874.
(35) Sumathi, R.; Carstensen, H. H.; Green, W. H. *J. Phys. Chem. A* **2001**, *105*, 6910.
(36) Sumathi, R.; Carstensen, H. H.; Green, W. H. *J. Phys. Chem. A* **2001**, *105*, 8969.
(37) Sumathi, R.; Carstensen, H. H.; Green, W. H. *J. Phys. Chem. A* **2002**, *106*, 5474.
(38) Saeys, M.; Reyniers, M. F.; Marin, G. B.; Van Speybroeck, V.; Waroquier, M. *AIChE J.* **2004**, *50*, 426.
(39) Saeys, M.; Reyniers, M. F.; Van Speybroeck, V.; Waroquier, M.; Marin, G. B. *ChemPhysChem* **2006**, *7*, 188.
(40) Sabbe, M. K.; Reyniers, M. F.; Van Speybroeck, V.; Waroquier, M.; Marin, G. B. *ChemPhysChem* **2008**, *9*, 124.
(41) Willems, P. A.; Froment, G. F. *Ind. Eng. Chem. Res.* **1988**, *27*, 1959.
(42) Willems, P. A.; Froment, G. F. *Ind. Eng. Chem. Res.* **1988**, *27*, 1966.
(43) Truong, T. N. *J. Chem. Phys.* **2000**, *113*, 4957.
(44) Zhang, S. W.; Truong, T. N. *J. Phys. Chem. A* **2003**, *107*, 1138.
(45) Baboul, A. G.; Curtiss, L. A.; Redfern, P. C.; Raghavachari, K. *J. Chem. Phys.* **1999**, *110*, 7650.
(46) Frisch, M. J.; Trucks, G. W.; Schlegel, H. B.; Scuseria, G. E.; Robb, M. A.; Cheeseman, J. R.; Montgomery, J. A., Jr.; Vreven, T.; Kudin, K. N.; Burant, J. C.; Millam, J. M.; Iyengar, S. S.; Tomasi, J.; Barone, V.; Mennucci, B.; Cossi, M.; Scalmani, G.; Rega, N.; Petersson, G. A.; Nakatsuji, H.; Hada, M.; Ehara, M.; Toyota, K.; Fukuda, R.; Hasegawa, J.; Ishida, M.; Nakajima, T.; Honda, Y.; Kitao, O.; Nakai, H.; Klene, M.; Li, X.; Knox, J. E.; Hratchian, H. P.; Cross, J. B.; Bakken, V.; Adamo, C.; Jaramillo, J.; Gomperts, R.; Stratmann, R. E.; Yazyev, O.; Austin, A. J.; Cammi, R.; Pomelli, C.; Ochterski, J. W.; Ayala, P. Y.; Morokuma, K.; Voth, G. A.; Salvador, P.; Dannenberg, J. J.; Zakrzewski, V. G.; Dapprich, S.; Daniels, A. D.; Strain, M. C.; Farkas, O.; Malick, D. K.; Rabuck, A. D.; Raghavachari, K.; Foresman, J. B.; Ortiz, J. V.; Cui, Q.; Baboul, A. G.; Clifford, S.; Cioslowski, J.; Stefanov, B. B.; Liu, G.; Liashenko, A.; Piskorz, P.; Komaromi, I.; Martin, R. L.; Fox, D. J.; Keith, T.; Al-Laham, M. A.; Peng, C. Y.; Nanayakkara, A.; Challacombe, M.; Gill, P. M. W.; Johnson, B.; Chen, W.; Wong, M. W.; Gonzalez, C.; Pople, J. A. *Gaussian 03, Revision C.02*; Gaussian, Inc.: Wallingford, CT, 2004.
(47) Scott, A. P.; Radom, L. *J. Phys. Chem.* **1996**, *100*, 16502.
(48) Katzer, G.; Sax, A. F.; Kalcher, J. *J. Phys. Chem. A* **1999**, *103*, 7894.
(49) Katzer, G.; Sax, A. F. *J. Phys. Chem. A* **2002**, *106*, 7204.
(50) Crosby, L. D.; Kurtz, H. A. *Application of electronic structure and transition state theory: Reaction of hydrogen with silicon radicals*; 46th Annual Sanibel Symposium, St Simons Island, GA, 2006.
(51) Martin, J. M. L.; de Oliveira, G. *J. Chem. Phys.* **1999**, *111*, 1843.
(52) McQuarrie, D. A.; Simon, J. D. *Molecular Thermodynamics*; University Science Book: Sausalito, CA, 1999.
(53) Hirschfelder, J. O.; Wigner, E. *J. Chem. Phys.* **1939**, *7*, 616.
(54) Pfaendtner, J.; Yu, X.; Broadbelt, L. J. *Theor. Chem. Acc.* **2007**, *118*, 881.
(55) Gupta, A.; Swihart, M. T.; Wiggers, H. *Adv. Funct. Mater.* **2009**, *19*, 696.
(56) Albu, T. V.; Lynch, B. J.; Truhlar, D. G.; Goren, A. C.; Hrovat, D. A.; Borden, W. T.; Moss, R. A. *J. Phys. Chem. A* **2002**, *106*, 5323.
(57) Wiberg, K. B. *Tetrahedron* **1968**, *24*, 1083.

JP9062516